CHAPTER 5

Cell Adhesion Measured by Force Spectroscopy on Living Cells

Martin Benoit

Center for Nanoscience
Ludwig-Maximilians-Universität München
D-80799 München, Germany

I. Introduction

Cell-to-cell adhesion is essential for multicellular development and arrangement. Cells may carry several different adhesion molecules (Kreis and Vale, 1999), resulting in a high variability of the molecular repertoire of the cell surfaces. This variability is reflected in the broad pattern of adhesion-controlled cellular functions during development and adult life (Fritz *et al.,* 1993; Springer, 1990; Vestweber and Blanks, 1999).

To determine cell adhesion many techniques have been evolved, such as functionalized latex beads moved with optical tweezers (Choquet *et al.,* 1997), microfluorescence assays or interferrometric techniques (Bruinsma *et al.,* 2000), and centrifugation experiments, e.g., with cell spheroids (John *et al.,* 1993; Suter *et al.,* 1998). Viscoelastic properties of cells were measured by cell poking and even with spatial resolution by an atomic

METHODS IN CELL BIOLOGY, VOL. 68

0091-679X/02 $35.00

force microscope (AFM) in either force modulation mode or more recently by force volume techniques (Domke *et al.*, 2000; Goldmann *et al.*, 1998; Hoh and Schoenenberger, 1994; Radmacher *et al.*, 1996; Zahalak *et al.*, 1990). Adhesion between single cells, e.g., granulocytes and target cells, was measured in the past using mechanical methods, such as micropipette manipulations (Evans, 1985, 1995) or hydrodynamic stress (Chen and Springer, 1999; Curtis, 1970). With the development of piconewton instrumentation based on AFM technology (Binnig *et al.*, 1986), the force resolution and the precision of positioning have allowed measurements at the single-molecule level (Gimzewski and Joachim, 1999; Müller *et al.*, 1999; Oesterhelt *et al.*, 2000). Forces for conformational transitions in polysaccharides (Marszalek *et al.*, 1999; Rief, Oesterhelt *et al.*, 1997) for the unfolding of proteins (Oberhauser *et al.*, 1998; Rief, Gautel *et al.*, 1997; Smith *et al.*, 1999) and for stretching and unzipping of DNA (Rief *et al.*, 1999; Strunz *et al.*, 1999) were measured. Unbinding forces of individual ligand–receptor pairs were determined (Baumgartner *et al.*, 2000; Florin *et al.*, 1994; Hinterdorfer *et al.*, 1996; Müller *et al.*, 1998) and the basic features of the binding potentials were reconstructed (Grubmüller *et al.*, 1995; Merkel *et al.*, 1999). Recently, the first steps toward cell adhesion measurements with AFM technology were made (Domke *et al.*, 2000; Razatos *et al.*, 1998; Sagvolden *et al.*, 1999).

Several theories have been developed to describe the processes which are involved while separating cells by either modeling single independent contacts or picturing more elaborate mechanisms such as molecular clustering (Evans and Ritchie, 1997; Kuo *et al.*, 1997; Ward *et al.*, 1994; Ward and Hammer, 1993).

In this section a new AFM-based experimental platform to investigate cell-to-cell interactions *in vivo* down to the molecular level will be described, immobilizing living cells to a force sensor. Epithelial cells (RL95-2 and HEC-2-A) from human endometrium as a substrate for an artificially rebuilt human trophoblast (JAR) are used to distinguish molecular adhesion processes involved not only in embryo–uterus interactions but also between individual cells of *Dictyostelium discoideum* to measure the adhesion force of single-contact site A proteins.

To obtain reproducible results, the complexity of living cells demands recording, estimating, and pinpointing a large variety of parameters. Therefore the contact-force is controlled down to 30 pN during the contact between well-studied cell types in a defined cell culture environment.

II. Instrumentation

The cell adhesion force spectrometer with an integrated optical microscope is specialized for force measurements on living cells. As a force sensor, a standard AFM cantilever is placed underneath a Perspex holder. The force signal is obtained from the deflection of the laser beam (Fig. 1) and plotted as force versus piezo position (e.g., Fig. 5). The spring constant of the cantilever in each experiment is determined using the thermal noise technique reported earlier (Florin *et al.*, 1995). By using sensors with a low spring constant, less force is applied to a cell when touched. The force resolution lies between 20

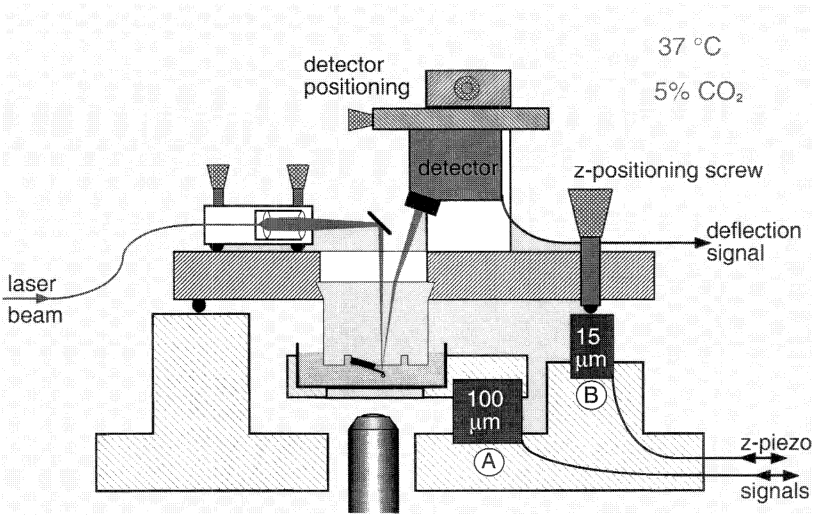

Fig. 1 Schematic of the adhesion force spectrometer with a light microscope below the Petri dish. The sensor mounted on a Perspex holder is placed from above in the Petri dish with the detecting laser unit. Two versions of cell adhesion force spectrometers: (A) long-range (100 μm) piezo moving the Petri dish and (B) short-range (15 μm) piezo moving the force sensor.

and 3 pN and is recorded together with the piezo position at a precision of 1 Å in either 256 pts (12 bit) or 32,768 pts (16 bit) per trace. The frequency of data collection is 60 kHz and the noise can be reduced by either filtering or averaging. For positioning, the sample is manually driven by an x-y stage mounted on a high-precision z piezo-actuator (100 μm)[1] with a strain gauge for long-range cell interactions (Thie *et al.,* 1998) (Fig. 1A). To detect shorter range interactions the Perspex holder is moved by a high-precision z piezo actuator (15 μm) which is equipped with a strain gauge (Dettmann *et al.,* 2000) (Fig. 1B). The z piezo velocity was typically set between 1 and 7 μm/s.

Slower velocities often interfere with drift effects basically caused by cell movement, while at higher velocities hydrodynamics influence the measurement. The lateral sample displacement is disabled during most of the experiments reported here. The approach of the sensor to the surface stops automatically if a certain threshold force is reached. This force can be kept constant within a certain range by a feedback loop compensating movements of the cells or piezo drift, especially if contacts last several minutes. Measurements are performed in an appropriate medium for living cells in a cell culture dish. To achieve long-time measurements standard cell culture conditions at 37°C in CO_2 (5% v/v) can be applied. The cells are monitored using the light microscope during the entire experiment.

[1]Especially nerve cells tend to form strongly adhering membrane tethers (Dai and Sheetz, 1998) over distances of millimeters. Even 100 μm is not enough to separate these cells from each other.

III. Preparations of the Force Sensor for Measurements with Living Cells

To immobilize cells on the force sensor without harming them is most crucial for operating the cell adhesion force spectrometer (Fig. 1). Here a single cell or, alternatively, a whole monolayer of epithelial cells will be immobilized to the sensor (Figs. 2A and 2B).

Since most cells express adhesion molecules on their surface, a very gentle method of immobilization is establishing a matching connection to these molecules.

A. Cell-Surface Adhesion Force Measurements

To determine which proteins to use for immobilizing the respective cells, as a first step, we characterized the adhesion forces by probing the cells with differently functionalized sensors. To distinguish the adhesion of the coating to be tested from the nonspecific interaction between surface and cell, a treatment had to be found to inactivate the sensor surface prior to applying the functionalizing molecules.

1. Immobilization of a Sphere to the Sensor

To better define the contact area between sensor and cells, a sphere of 60 μm in diameter from either sephacryl or glass is fixed at the end of a cantilever. The spheres are mounted to the cantilevers (DNP-S Digital Instruments, Santa Barbara, CA; or Microlever, Park Scientific Instruments, Sunnyvale, CA) in the following manner.

A tiny spot of epoxy glue (UHU plus endfest 300, Bühl, Germany) is applied to the tip of a cantilever using a patch-clamp glass electrode. Then a single Sephacryl S-1000 sphere (Pharmacia, Freiburg, Germany) or a glass sphere (G 4649; Sigma, Deisenhofen/Germany), about 60 μm in diameter, which sticks electrostatically to a cannula (Terumo No. 20, Leuven/Belgium) is placed on the epoxy. To cure the epoxy, the microsphere-mounted cantilever is then heated at 90°C for 45 min. Another method is described in Holmberg *et al.* (1997). Before use, the cantilevers were sterilized in 70% ethanol for 2 h and washed thoroughly in distilled water. Sensor tips and spheres fixed to the force sensor (Fig. 3) with various coatings were tested on the cells of interest.

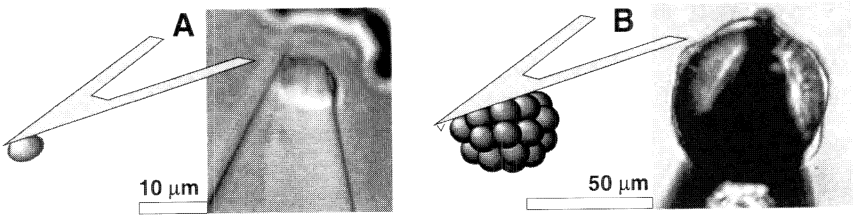

Fig. 2 Schematics and light microscopic image of (A) a single-cell (*Dictyostelium discoideum;* the cells on the cover slide are out of focus) and (B) a layer of cells (osteoblasts) on a glass sphere immobilized on a force sensor.

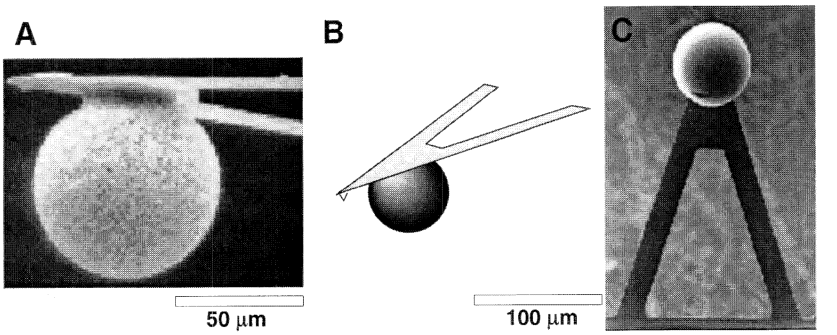

Fig. 3 Schematics (B) and images of a sephacryl (A) and a glass (C) sphere (diameter 60 μm) glued to a force sensor.

2. Passivated Force Sensors

The following protocol, derived from Johnsson *et al.* (1991), proved useful for preparing sensors with a sufficiently low nonspecific interaction with cells.

First the Si–OH layer of either a SiO_2 or a Si_3N_4 surface is ammino-silanized with *N*′-(3-(trimethoxysilyl)-propyl)-diethylentriamin (Aldrich) at 80°C for 10 min to obtain an amino-functionalized surface. It is then washed in ethanol and completely crosslinked for 10 min in water at 80°C. A phosphate-buffered saline (pH 7.4) (PBS Sigma) solution of 10 mg/ml of carboxymethylamylose (Sigma) is activated with 20 mg/ml *N*-hydroxysuccinimide (NHS, Aldrich) and 20 mg/ml 1-ethyl-3-(3-dimethylaminopropyl)carbodiimide (EDC, Sigma) for 2 min. The tip is then incubated with the NHS-activated amylose for 15 min, rinsed three times in PBS, incubated with 0.5 mg/ml ethanolamine (Sigma) in PBS for 1–2 h, and intensively rinsed in PBS. Other preparation techniques with PEG have also proved to sufficiently passivate surfaces for proteins and cells (Bruinsma *et al.*, 2000; Willemsen *et al.*, 1998).

3. Results

From the "deadhesion force versus piezo position traces" (e.g., Fig. 4 or Fig. 5) adhesion can be characterized in an initial approach by measuring the maximum adhesion force. As shown later, other adhesion parameters will be derived from these traces. If a sphere is lowered onto a soft cell surface, the area of interaction increases with the indentation which leads to an enhancement of the adhesion signal. The adhesion strength is not only dependent on the indentation force (here 3 ± 1 nN) while the cells are brought and held in contact as mentioned earlier but also, as shown in Fig. 5, on the duration of the contact. This is probably due to the fact that the cell shape adapts to the sphere's surface and more and more molecules can interact with this surface with time. The adhesion to the sepacryl spheres is enhanced by at least 50% compared to that to a glass sphere, in agreement with their structured and therefore larger surface. Changing the velocity of retraction leads to a fairly linear relation between separation speed and adhesion in the range between 2 and 27 μm/s. However, for low velocities the influence

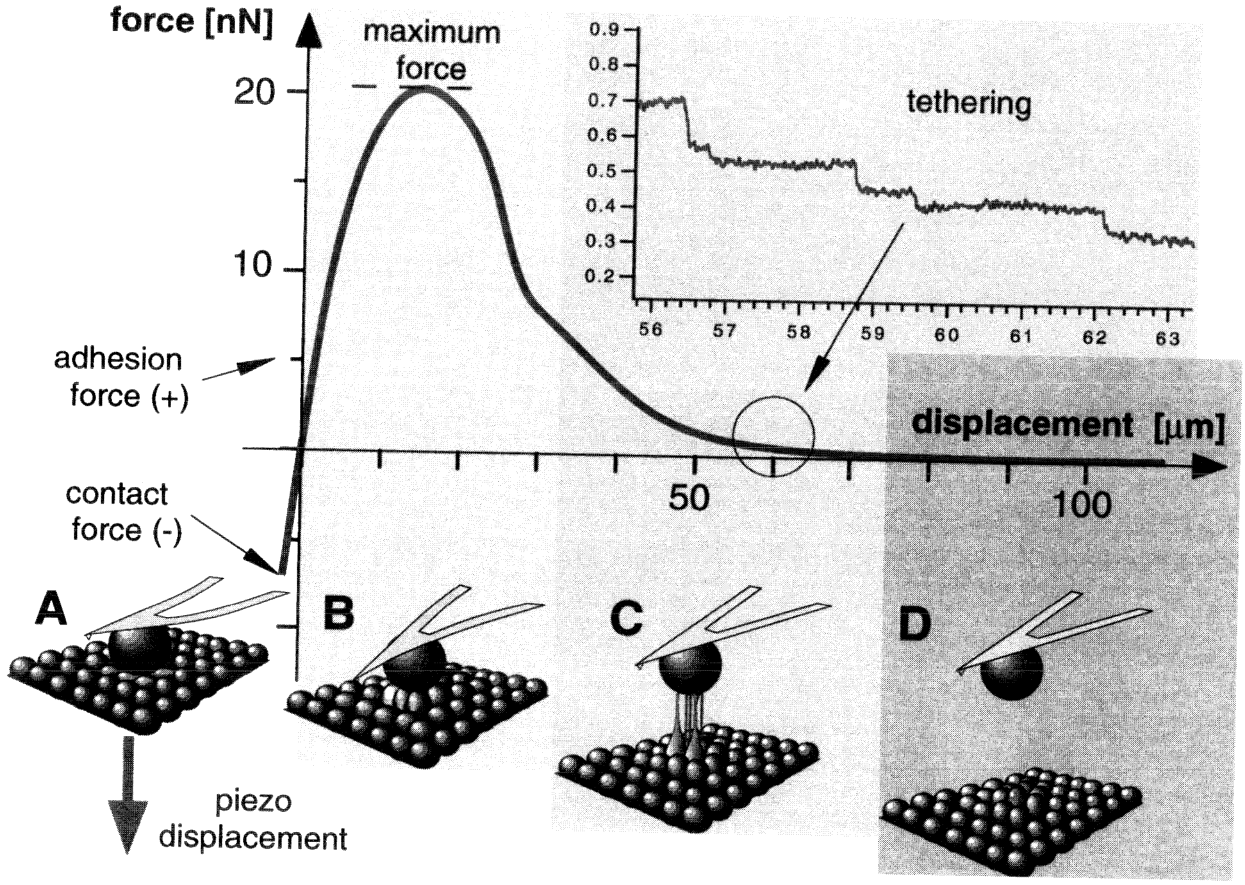

Fig. 4 A typical force versus piezo displacement trace on an epithelial cell layer with schematics of the experimental situation of the cell contact (A), the maximum force regime (B), the tethering regime (C), and the complete separation (D). Contact force indicated with negative values and adhesion force (sensor is elongated downwards) indicated with positive values.

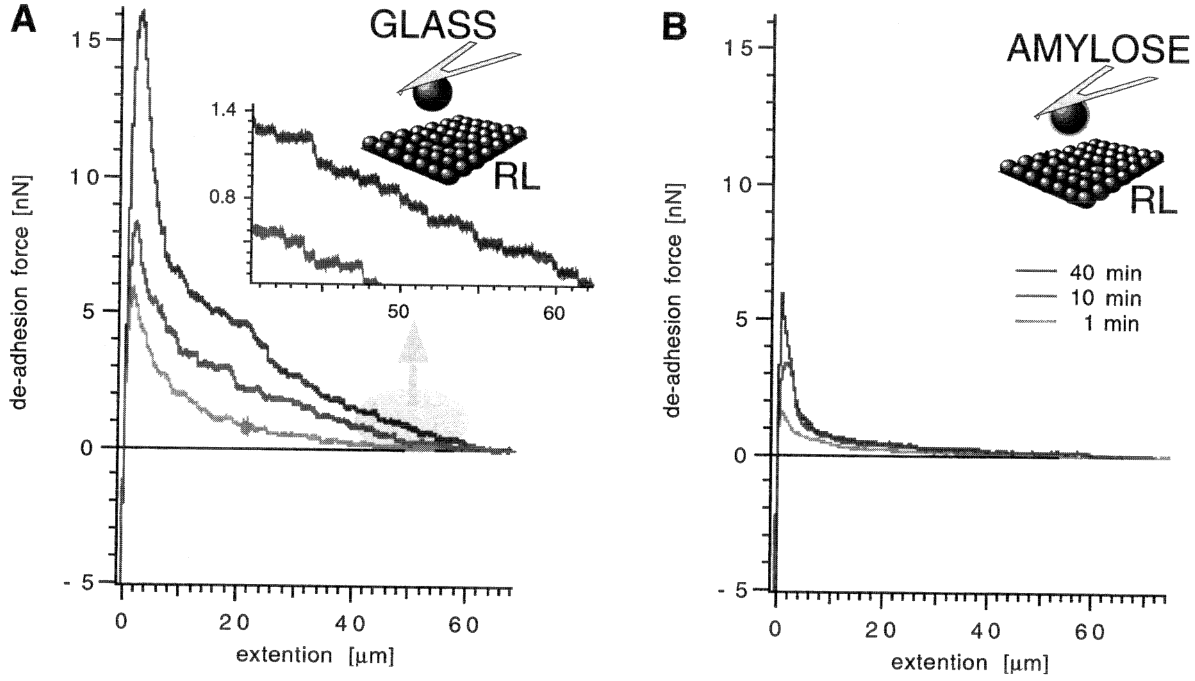

Fig. 5 Two sets of deadhesion force traces recorded with a plain glass surface on the sensor (A) and an amylose-passivated surface (B) after contacts of 1, 10, and 40 min at 5 nN on a confluent monolayer of epithelial cells (RL95-2). The contact area was about 500 μm^2. Inset (A) zooms into the traces where indicated by the circle revealing single rupture steps (Thie *et al.*, 1998). (See Color Plate.)

of the cells on both laser reflex and drift becomes prominent, whereas for high velocities hydrodynamics come into play. To compare the results from different experiments in all the measurements with spheres presented here, the velocity was held constant at 7 μm/s.

Scrutinizing the deadhesion force curves more closely one will find more or less pronounced single steps in the order of 100 pN in the regions of descending adhesion (inset of Fig. 5A) indicating ruptures on the molecular level. Counting them could give a very rough estimate on the number of molecules involved. But unfortunately these steps are only resolved in the descending shoulder of the traces far away from the maximum force.

Nevertheless the results shown in Fig. 5 clearly point out the passivation of the originally adhesive glass surface with amylose even for long contact times.

Carboxymethylamylose also can be used for crosslinking certain molecules to specifically activate the passivated surface. Before saturating the amylose with ethanolamine, a protein with a NH_2 group can be bound covalently to the carboxy groups of the amylose activated with EDC and NHS.

4. Specifically Functionalized Force Sensors

Protein is immobilized on the sensor surface by carboxy-methylated amylose (Grandbois *et al.*, 1999; Johnsson *et al.*, 1991). Alternatively the surface treatment with PEG by Hinterdorfer *et al.* (1996) is recommended for such activations (Willemsen *et al.*, 1998). Initially the sensor is functionalized in the same way as described earlier: First, the standard commercially available Si_3N_4 cantilevers (with glass beads) are silanized. Second, 10 mg/ml of carboxymethylamylose is activated with 2–10 mg/ml NHS and 5–10 mg/ml EDC[2] for 1–5 min in PBS solution. As described earlier, the sensor is incubated with the activated amylose for 10–15 min. After rinsing three times in PBS it is immediately incubated with 0.05–0.5 mg/ml of the molecule of interest in PBS for 2 h—optionally fresh EDC and NHS have to be added with the molecule if there is a time delay of more than 15 min. The only restriction to this molecule is that it must favorably exhibit an exposed NH_2 group, preferably far away from its binding pocket.[3] Intensive rinsing in PBS removes the unbound molecules.

5. Results and Discussion

It is now, for instance, possible to probe a cell surface by an AFM tip specifically functionalized with a lectin (Grandbois *et al.*, 2000). This technique might be used to monitor locally the time course of extracellular membrane molecule expression because it is harmless to the cells and does not block the receptors by labeling. With this setup various molecules were tested for their ability to immobilize cells on a sensor. Even though there are differences in adhesion between the various cell types, in general, the spontaneous adhesion, after short contact periods of less than a minute, either to NH_2 groups of just amino-silanized spheres or to aldehyde groups was found to be extremely

[2]For lower concentration the free segments of the amylose chain become longer.

[3]If the binding pocket is potentially inactivated by binding the amylose with NH_2 groups too close to the pocket, a soluble binding partner lacking any NH_2 groups could be added during activation to protect the binding site. The ligand must then be washed out carefully before the experiment.

strong for all cells at the initial contacts. But the adhesion decreased very rapidly with each additional experiment, especially when measuring in nutrient medium with protein-rich additives, indicating that the reactive groups were saturated irreversibly with bound molecules. Lower adhesion strengths were measured for certain lectins, such as either wheat germ agglutinin (WGA, Sigma) or concavalin A (con A, Sigma), which bind to the glycocalyx of assigned cells. Due to the lectins' specificity to certain glycoproteins, they were not significantly affected by nutrient medium and did not lose their ability to bind. In addition they self-cleaned due to their offrate (10^{-3-5}/s) if free molecules were caught in the binding pocket.

In measuring adhesion on epithelial cells, one must consider their habit to polarize. Thus, in a monolayer, epithelial cells differ among other properties in the proteins expressed on both the apical (free) membrane and the membranes presented to the substrate or to their neighbors. Interestingly, even the spontaneous adhesion of epithelial cells—whose apical surface is not supposed to adhere—to plain cantilevers or glass surfaces is still prominent: however, it does not differ much from measurements on surfaces functionalized by BSA, or just incubated in polylysins, fibronectin, or laminin (data not shown). Since this adhesion is independent of the coating, it is assumed to be a non-specific surface interaction, whereas this "nonspecific" adhesion of single *Dictyostelium discoideum* cells e.g. to the plain force sensor (data not shown) is useful for locomotion or ingestion.

B. Adhesion Force Measurements between Cell Layers

To apply this technique to force measurements between epithelial cell layers (epithelium) the already well-investigated human embryo–uterus interaction was chosen. JAR cells represent the invasive trophoblast, RL cells, and the receptive uterine epithelium. From centrifugation experiments (John *et al.,* 1993) HEC cells are supposed to represent the nonreceptive uterine epithelium.

1. Immobilizing a Monolayer of Cells to a Force Sensor

Before seeding cells, the sensor is carefully rinsed in alcohol and water, precoated with polylysins, laminins, fibronectins, or other adhesive coatings,[4] and placed upside-down in nutrient medium.

Of course surface passivation is neither helpful for seeding cells nor necessary, since the whole surface will be covered with cells. To grow a monolayer of cells on a force sensor and to predefine the later contact area, it is also useful to glue either a glass or, better, a sephacryl sphere underneath the cantilever as described earlier. Then a drop of suspended cells is released onto the sphere (Fig. 6). From time to time (3–14 h) this procedure is repeated until one or more cells are attached to the sphere. Cells growing on the sensor arms are not found to disturb the experiments as long as they neither move nor cover the part of the sensor where the detecting laser beam is reflected. Even then, measurements are possible although occasionally suspicious malformed traces should

[4]We recommend using the customary surface treatment techniques for the force sensor's surface because the cells must grow on the surfaces for several days until a proper monolayer is established.

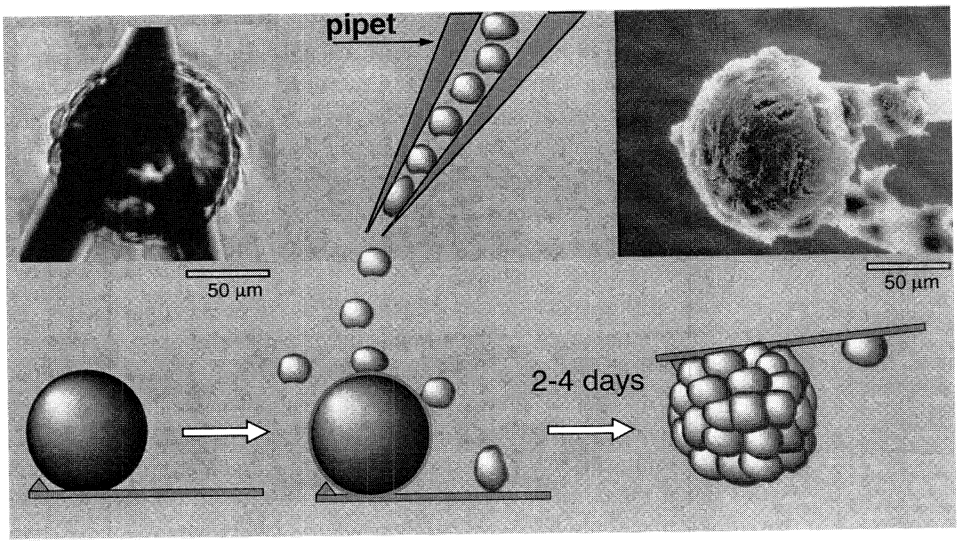

Fig. 6 Schematic of growing cells on a sensor sphere [developed by R. Röspel (Thie *et al.*, 1998)]. The result is shown as an LM image and a SEM image.

be neglected.[5] Vesicles or other cellular compartments, which tend to disturb the laser beam, easily contaminate the fluid when working with living cells. Therefore the medium should be exchanged freshly several times before starting the measurement.

When the cells finally cover the sphere confluently, the lever is placed in the force spectrometer and moved onto a surface of interest.

With such prepared sensors (Fig. 6) several surfaces (e.g., potential implants) can either be probed or, as shown here, be used to investigate certain aspects of embryo–uterus interactions.

With this preparation, the mechanisms of the interaction between human trophoblast-type JAR cells (JAR) with the two human uterine epithelial cell lines RL95-2 (RL) and HEC-1-A (HEC) were investigated. RL cells, in contrast to HEC cells, are supposed to respond to the contact with JAR cells in a specific way (John *et al.*, 1993; Thie *et al.*, 1997, 1998).

2. Results

JAR-coated force sensors were brought into contact with confluent monolayers of HEC and RL cells. Figure 7 shows de-adhesion force curves for the different cell types after various contact duration. Despite the variation of the de-adhesion curves due to the various radii of the spheres (65 ± 10 μm) and some cells occasionally disturbing the

[5]To be on the safe side, one could think of passivating the sensor prior to gluing the sphere, but this might affect the strength of the epoxy glue.

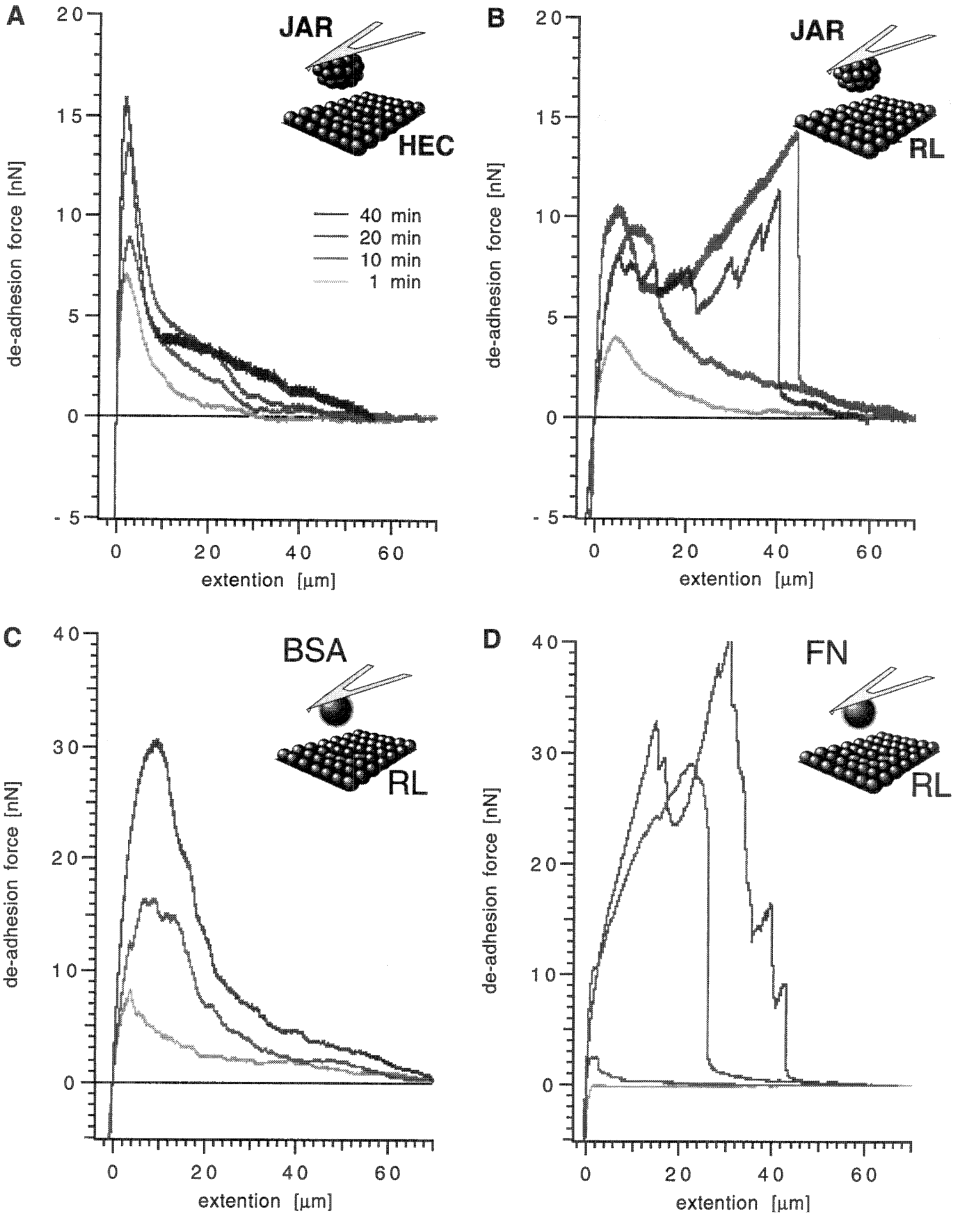

Fig. 7 Typical adhesive force curves for (A) HEC-1-A and (B) RL95-2 cells resulting when a JAR-coated sensor, (C) a bovine serum albumin (BSA)-coated sensor, or a (D) fibronectin (FN)-coated sensor is retracted after periods of 1–40 min time of contact at approximately 5 nN (Thie *et al.,* 1998).

Table I
Listing of JAR Experiments[a]

	HEC/JAR		RL/JAR	
Time (min)	Continuous	Discontinuous	Continuous	Discontinuous
1	87	0	154	0
10	55	0	67	0
15	24	0	38	0
20	24	0	19	5[b]
30	11	0	6	4
40	13	0	5	14[b]

[a]HEC never showed discontinuous deadhesion, while RL does.
[b]After one of these experiments, a cell was found loosened on the monolayer.

laser reflex, typical features can be recognized. As in Fig. 5, the adhesion increases with increasing contact time in Fig. 7. For contact times of less than 20 min, the response of both cell types is virtually indistinguishable within the experimental error of the variations between different preparations. However, for prolonged contact duration, the two cell types (Fig. 5A HEC, Fig. 5B RL) showed a marked difference in the deadhesion profile. This difference becomes particularly prominent after the maximum adhesion force. Here, the contact between JAR and RL cells was found to be significantly different from JAR and HEC cells, since the de-adhesion often propagates discontinuously after cell contacts of at least 20 min. The force builds up upon separation until the cells detach with remarkably large force steps from 0.5 to far more than 5 nN (Table I), while the force between JAR and HEC decreases continuously in small steps (inset Fig. 5A) of less than 200 pN upon separation in all cases.

It has been previously postulated that there is a local cross-talk between trophoblast and uterine epithelium leading to specific cell–cell binding, i.e., a redistribution/upregulation/activation of adhesion systems at the free cell pole (Albers *et al.,* 1995; Denker, 1994; Thie *et al.,* 1995, 1996). In this context, it is of interest that a discontinuous JAR–RL interaction is observed only after prolonged contact of both partners. This could be due to the time needed to build up cooperative islands of interacting adhesion molecules (molecular clusters). In contrast, the initial interaction observed after short contacts (<20 min) is caused by adhesion of independently adhering molecules.

To simulate this independent (noncooperative) adhesion mechanism, we probed both RL and HEC cells with pure spheres and spheres that were coated with bovine serum albumin (BSA) at different contact times. Since none of these experiments ($N = 250$) show the significantly discontinuous de-adhesion, they should reproduce, solely, the noncooperative molecular interactions. Figure 7C shows a typical set of the resulting de-adhesion curves for various contact times. As can be seen, there is very good agreement with the detachment traces recorded for HEC cells. But discontinuous de-adhesion at prolonged contact times is no longer detectable.[6] An experiment equivalent to JAR spheres

[6]Notable is the increased maximum adhesion compared to the measurement in Fig. 5A due to the fact that here a sephacryl sphere was coated with BSA and not a glass sphere.

on RL monolayers, carried out with a fibronectin-coated sphere (with reduced adhesion background by the amylose), also results in discontinuous de-adhesion in 14 of 20 sets (as can be seen in Fig. 7D). As in the case of the JAR–RL interaction after long cell contacts, the discontinuous de-adhesion signature appears only after contacts for more than 20 min. On the contrary, the noncooperative adhesion of the FN spheres is drastically reduced for short contact duration, but the FN reaction is enhanced[7] compared to the measurements on JAR/RL after long contacts. Since RL cells are known to interact with JAR cells via fibronectin-binding proteins (certain integrins; Thie and Ramunddal, unpublished data), these experiments corroborate our assumption that this discontinuous adhesion is due to a specific interaction. This conclusion is supported by previous work of other groups which had investigated integrin–cytoskeleton interactions in other cell types where integrin–ligand binding promotes redistribution of the integrins to molecular clustering (Felsenfeld *et al.,* 1996; Yauch *et al.,* 1997).

3. Discussion

The first set of findings here demonstrates that force spectroscopy is a technique, which allows the uncovering of contact time-dependent adhesion processes and the scrutinization of specific receptor-mediated interactions as well as nonspecific cell–cell or cell–substrate adhesion.

The adhesion to sephacryl spheres after some minutes of contact with cells (which is identical to BSA-coated sephacryl spheres Fig. 7D) is rather high compared to that to glass spheres. The cells may gain adhesion strength when creeping into the structured surface (Fig. 3A) of the sephacryl spheres enlarging the interacting area and possibly snatching the hooks and grips. These surfaces are then good for culturing cells on them, but for passivation smooth surfaces like glass are recommended. The adhesion between JAR and HEC is in most cases slightly higher than that between JAR and RL which might be due to the larger surfaces of the microvilli-rich HEC cells. Assumably the cell body becomes elongated in the ascending part of the deadhesion trace until the cytoskeleton is stretched out after 10–20 μm depending on the thickness of the layers and the type of cells. In the region of maximum force the likelihood of braking adhesion links due to the large load is very high. The interconnection does not break up to 80 μm despite overstretching the cells further than 40 μm, indicating an adhesion concept which does not include the cytoskeleton. The membrane tethers must mediate this adhesion, as visible by the characteristic step pattern indicating single de-adhesion events on the molecular level. The small slope prior to the stepwise ruptures also confirms the presence of tethers in this region. Here the HEC cells show a larger tendency to form tethers due to the microvilli-rich surface compared to the smoother surface of RL cells. Tether formation in the case of RL/JAR cells after long contacts is outranged by the strong adhesion concept[8] of cooperating molecules clustering in adhesion islands. Furthermore, from

[7]Even though using passivated glass spheres, the adhesion is significantly higher than all other measurements, probably due to high density of fibronectin on the surface.

[8]Despite the fact that in the LM no damages of the cells could be resolved, the fact that in three cases single cells were found pulled out from the monolayer suggests an injury of the membranes after such strong de-adhesion events.

the fact that the adhesion forces increase after the first force maximum upon further stretching prior to the ruptures, an involvement of the cytoskeleton must be considered.

The embryo passing to the site of implantation always stays in contact with cells of the guiding tissue, i.e., oviductal and uterine epithelium. This can be guaranteed by the adhesion concept of the tethers (Chen and Springer, 1999) as shown by the JAR/RL adhesion measurements. Slow movement of the sphere is also provided, since the adhesion forces of former contacts disappear while moving away while new connections are formed in the direction of motion. During this "damped walk" the cells have time to "communicate" and to form strong adhesion clusters when the target area is reached. Then the force increases when trying to move farther—the motion will be stopped by this adhesion concept as shown by the JAR/RL adhesion measurements.

C. Cell–Cell Adhesion Force Measurements

We will now consider the interaction between single cells by combining single-molecule force spectroscopy with genetic manipulation for the measurement of de-adhesion forces at the resolution of individual cell-adhesion molecules. In general single cells behave different from cells in tissue. But, to resolve single-molecule events instead of cooperative molecular effects, it is necessary to minimize contact area, contact time, and contact force. Two steps in the refinement of the technique are crucial for measuring discrete de-adhesion forces at molecular resolution: (i) reduction of the contact force which results in a further decrease of the contact area and (ii) shortening of the contact time which reduces the number of contacts established. The cell adhesion force spectrometer is therefore able to control the contact force down to 30 pN when using soft cantilevers (5 mN/m). A single cell on the cantilever reduces the contact area to a minimum. The measurements focus on contact site A (csA) as a prototype of cell adhesion proteins. The csA glycoprotein is specifically expressed in aggregating cells of *Dictyostelium discoideum* which are engaged in the process of building up a multicellular organism.

The eukaryote *D. discoideum* offers the advantage that one particular type of adhesion molecule, the developmentally regulated (csA) glycoprotein, can be singled out by genetic manipulations (Faix, 1999). In *D. discoideum,* csA participates in cell aggregation, the transition from the single-cell to the multicellular stage (Ponte *et al.,* 1998). Thus, csA is undetectable in growth-phase cells but is expressed upon starvation (Murray *et al.,* 1981). In developing cells of the aggregation stage, csA covers roughly 2% of the total cell surface area (Beug, Katz, and Gerish, 1973). CsA molecules react with each other (homophilic interaction), forming noncovalent bonds linking the surfaces of adjacent cells (Kamboj *et al.,* 1988), which are anchored in the plasma membrane by a ceramide-based phospholipid (Stadler *et al.,* 1989).

1. Immobilizing a Single Living Cell to a Force Sensor

As shown by Razatos *et al.* (1998) even bacteria can be fixed to an AFM tip. With an appropriately functionalized force sensor, a living cell loosely sitting on a cell culture dish is tethered to the sensor (see following). Therefore the very end of the lever is lowered

onto the cell at a force of a few nanonewtons and held in contact for approximately 30 s to allow the specific molecules on the lever to bind before lifting the cell off the bottom of the dish. When the cell sticks to the sensor, it can be moved to a cell or surface of interest. Typically, the interaction strength between cell and cantilever increases with time, due to the assimilating cell surface. If the cell on the dish already sticks to the substrate too strongly, it can be pushed gently from the side with the edge of the lever before lifting it up. It would be helpful if at least the z piezo could be moved manually for this purpose. The best results were obtained with tipless cantilevers, as the tip either is likely to interfere with the adhesion measurements if it surmounts the cell or hinders the cell adhesion. Unfortunately, the spring constants of commercial tipless cantilevers are very stiff (Digital Instruments, 60 mN/m) compared to the soft cells (Radmacher, 1997). To obtain compliant and tipless force sensors, the cantilevers had to be modified destructively with thin tweezers, as follows, prior to functionalization. A curvature on one of the tweezers' fingers (Fig. 8) effects a grinding while gently squeezing the cantilever between the tweezers.

2. Results

As described previously, a *Dictyostelium* cell is picked up with a tipless AFM cantilever whose end had been covalently functionalized with wheat germ agglutinin (WGA lectin, Sigma). A target cell resting at the bottom of a Petri dish is positioned under the cell on the cantilever and approached until a predefined repulsive contact force is established (Fig. 9). This contact force is held constant for a defined time interval to allow cell adhesion to become established.

Force traces of the de-adhesion process between the two cells are shown in Fig. 10. A trace, typical of growth-phase cells that had been allowed to interact for 20 s at a contact force of 150 pN, is shown at the bottom of Fig. 10A. The adhesion between these cells gave rise to unbinding forces on the order of 1 nN, caused by several molecular

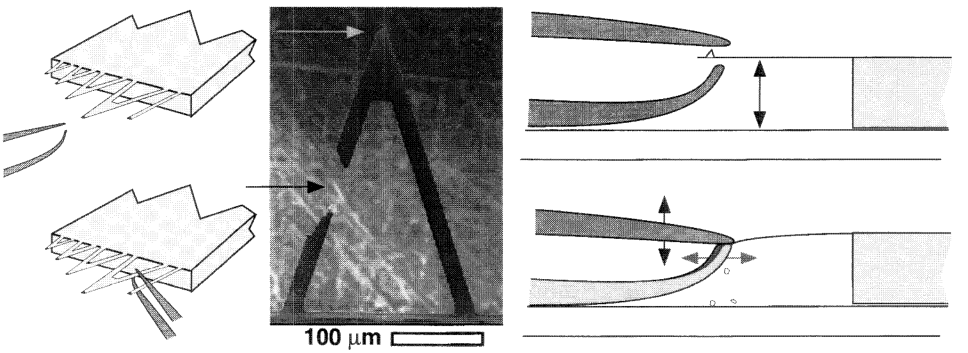

Fig. 8 Scheme of the "surgery" on a cantilever with tweezers and a SEM image of such a sensor. (See Color Plate.)

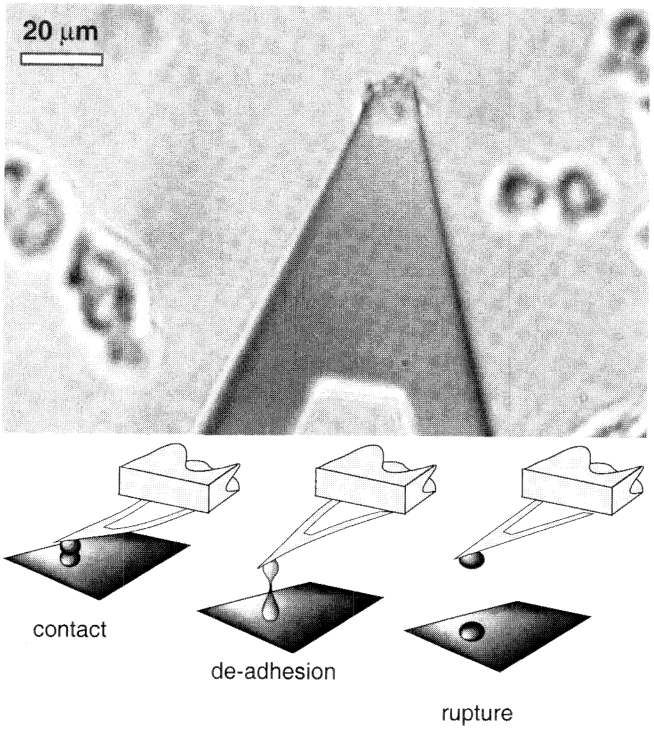

Fig. 9 Light microscopic image of a single cell on the sensor (cells on the surface are out of focus) and schematics of a force experiment (Benoit *et al.*, 2000).

interactions. Particularly in the last part of this deadhesion force trace the typical pattern for tether formation appears (Hochmuth *et al.*, 1996). Adhesion of the nondeveloped cells used in this experiment is known to be Ca^{2+} dependent (Beug, Katz, Stein, *et al.*, 1973). To test this Ca^{2+} sensitivity, 5 m*M* EDTA, a chelating agent, was added to the buffer. As illustrated (at the bottom of Fig. 10B) the adhesion is drastically reduced. Within the duration of the experiments this low amount of EDTA did not affect the cells' integrity. Since the cells tend to move on the surface of the dish it is necessary to check the cell contact by the built-in light microscope and readjust the positioning of the cells.

After growth-phase cells were brought together by contact forces of 30–40 pN applied for only 0.2 s, less than 20% of the de-adhesion traces showed binding between the cells (Fig. 10A). The histogram of the deadhesion forces showed a broad distribution with a maximum at about 50 pN. The low frequency of these de-adhesion events implies that, based on Poisson statistics, more than 90% of the contacts should reflect single binding events. Thus, the width of the force distribution most likely reflects a multitude of molecular species involved in the Ca^{2+}-dependent adhesion. In the presence of 5 m*M* EDTA, 96% of the cells did not establish detectable adhesion within 0.2 s, even when they were brought into contact with an increased force of 90 pN (Fig. 10B). On the basis

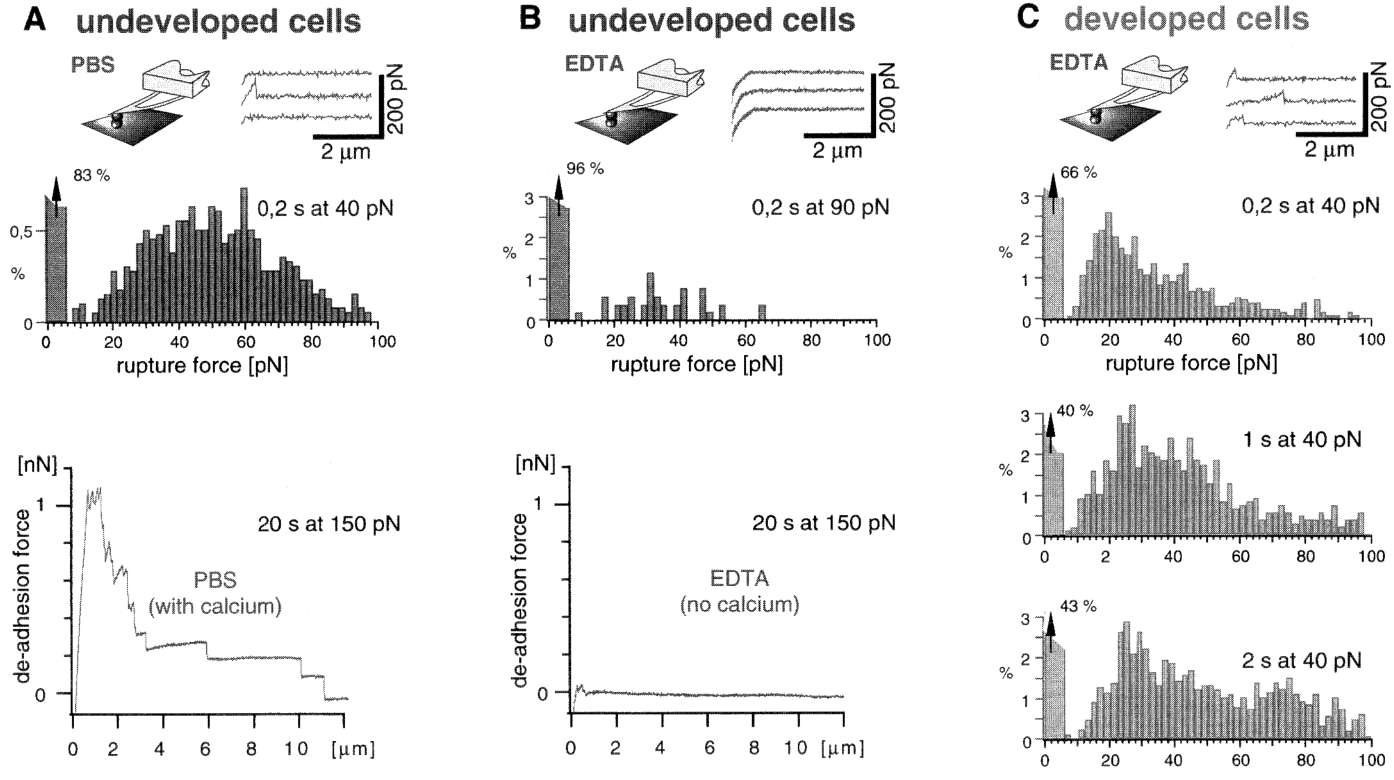

Fig. 10 Undeveloped cells lacking the CSA molecule express several Ca^{2+}-dependent adhesion molecules (A+B). Experiments in PBS (A) result in a typical rupture force spectrum derived from 5760 traces (inset) after contact for 0.2 s at 35 pN. Below: a representative trace from a prolonged contact for 20 s at 150 pN. Experiments in 5 m*M* EDTA (B) result in a force spectrum with reduced adhesion (only 4%) from 960 traces (inset) even though there was an increased contact force of 90 pN for 0.2 s. The prolonged contact for 20 s at 150 pN (below) does not show significant adhesion. Experiments in EDTA with developed cells (C) in contrast show typical force spectra for the CSA molecule. For 0.2 s at 35 pN, one peak at 20 pN becomes prominent from 1334 traces (inset). After contact for 1 s, the spectrum derived from 1088 traces (not shown) raises a second peak around 45 pN, and after 2 s, a third peak at 74 pN appears from 1792 traces (not shown) (Benoit *et al.*, 2000).

of these data, de-adhesion forces were measured in developing cells in which additional cell adhesion proteins are expressed. Cells in the aggregation stage are distinguished from growth-phase cells by EDTA-stable cell adhesion (Beug, Katz, and Gerish, 1973). When 5 m*M* EDTA was added to these cells and de-adhesion forces were determined after a contact force of 35 ± 5 pN, binding was observed in roughly half of the traces. The collection of traces shown in Fig. 10C illustrates the type of results obtained at various contact times. Often initial forces rose up to several hundred piconewtons, and unbinding occurred in several steps until the last tether connecting the two cells was disrupted at long contacts. In contrast to these multiple de-adhesion events, single steps of deadhesion prevailed after a contact time of 0.2 s.

The last force step, the one that completely separated the cells, was measured in more than 1000 traces after contact times of 2, 1, or 0.2 s (Fig. 10C). When these data were compiled in histograms, a pronounced peak indicating a force quantum of 21 ± 5 pN became apparent. Upon increasing of contact times from 0.2 sec to 2 sec, this peak only negligibly shifted to higher de-adhesion forces (23 pN). The main difference between the histograms resided in the lower contribution of higher forces upon the reduction of contact time. The higher forces contributing to de-adhesion after 2 or 1 s of cell-to-cell contact are interpreted as superimposed multiples of a basic force quantum of 23 pN.

Developmental regulation and EDTA resistance suggest that the measured force quantum of 23 pN is due to the unbinding of csA molecules. However, cells in the aggregation stage differ from growth-phase cells not only in the csA protein but also in several other developmentally regulated cell surface proteins. Therefore, to attribute the peak of 23 pN to the presence of this particular cell adhesion protein, different types of cells in which specifically csA expression was genetically manipulated were employed (Benoit *et al.,* 2000). The csA gene was selectively inactivated by targeted disruption using a transformation vector that recombined into the gene's coding region (Faix *et al.,* 1992). Only 25% of the cells in this csA knock-out strain showed measurable de-adhesion forces as compared to 86% of wild-type cells. Also, cells of a mutant unable to produce csA (Harloff *et al.,* 1989) were transfected with vectors that encode the csA protein under the control of the original promoter. Indeed these "repaired" cells showed adhesion like the wild-type only when developed. Together these results demonstrate that the csA molecule is the primary source of the intercellular adhesion measured by force spectroscopy in the presence of EDTA.

3. Dicussion

The quantized de-adhesion force of 23 pN indicates discrete molecular entities as the unit of csA-mediated cell adhesion. The most likely interpretation of this peak is that one unit reflects the interaction of two csA molecules, one on each cell surface. Nevertheless, since oligomerization may strongly increase the affinity of cell adhesion molecules (Tomschy *et al.,* 1996), we cannot exclude the possibility that defined dimers or oligomers represent the functional unit of csA interactions (Baumgartner *et al.,* 2000; Chen and Moy, 2000).

The measured de-adhesion force of 23 pN for csA is small compared to that of most antibody–antigen or lectin–sugar interactions, which frequently exceeds 50 pN at comparable rupture rates (Dettmann *et al.,* 2000). These moderate intermolecular forces involved in cell adhesion are consistent with the ability of motile cells to glide against each other as they become integrated into a multicellular structure. Moreover, in view of the limited force that the lipid anchor may withstand, much higher molecular unbinding forces would be of no advantage.

Here the separation rate was kept constant at 2.5 μm/s, resulting in force ramps between 100 and 500 pN/s depending on the elasticity of the cells. This rate is on the same order as the protrusion and retraction rates of filopods, the fastest cell surface extensions in *Dictyostelium* cells. With their adhesive ends, the filopods can act as tethers between cells or between cells and other surfaces. Our measurements of separation forces are therefore representative of upper limits to which the cells are exposed by their own motility.

IV. Cell Culture

A. HEC/RL Cell Culture on Coverslips

Measurements on human endometrial cell lines, purchased from the American Type Culture Collection (ATCC, Rockville, MD/USA), i.e., HEC-1-A (short HEC; HTB 112; (Kuramoto *et al.,* 1972)) and RL95-2 (short RL; CRL 1671 (Way *et al.,* 1983)), were performed in JAR medium at 36°C and 5% CO_2. For routine culture, cell lines were grown in plastic flasks in 5% CO_2–95% air at 37°C.

In brief, HEC cells were seeded out in McCoy's 5A medium (Gibco-Life Technology, Eggenstein, Germany) supplemented with 10% fetal calf serum (Gibco); RL cells, in a 1 + 1 mixture of Dulbecco's modification of Eagle's medium and Ham's F12 (Gibco) supplemented with 10% fetal calf serum, 10 m*M* Hepes (Gibco), and 0.5 μg/ml insulin (Gibco). All media were additionally supplemented with penicillin (100 IU/ml; Gibco) and Streptomycin (100 μg/ml; Gibco). The growth medium was changed every 2 to 3 days, and cells were subcultured by trypsinization (trypsin–EDTA solution; Gibco) when they became confluent. For experiments, cells were harvested by trypsinization from confluent cultures, counted, and adjusted to the desired concentration, i.e., RL95-2 700,000 cells and HEC-1-A 200,000 cells each in 2.0 ml of their respective culture medium (Fig. 2A and 2B). Subsequently, suspended cells were poured out on poly-D-lysine-coated glass coverslips (12 mm in diameter) situated in 4 cm^2 wells. Cells were grown in medium to confluent monolayers and transferred into a Petri dish before used for experiments.

B. JAR Cell Culture on Cantilever

Cantilevers mounted with sephacryl microspheres, as described earlier, were immersed in 0.01% poly-D-lysine for 1 h at room temperature, washed in medium several times,

and subsequently incubated with a human JAR choriocarcinoma cell suspension (ATCC: HTB 144 (Patillo *et al.,* 1971)) (200,000 cells/ml RPMI 1640 medium, Gibco, supplemented with 10% fetal calf serum and 0.1% glutamine). After JAR cells had settled, these cantilever–cell combinations were incubated in 5% CO_2–95% air at 37°C. Usually 3 to 4 days after the start of the cultures, cells were grown to confluency and cantilevers were ready to be used for the experiments.

C. *Dictyostelium* Cell Culture

All mutants were derived from the *D. discoideum* AX2-214 strain, here designated as wild-type. Mutant HG1287 was generated by E. Wallraff (Beug, Katz, and Gerish, 1973). In mutant HG1287, csA expression was eliminated by a combination of chemical and UV mutagenesis. In this mutant not only the csA gene but also other genes may have been inactivated by this shot-gun type of mutagenesis. Cells were cultivated in nutrient medium as described (Malchow *et al.,* 1972) in Petri dishes up to a density of 1×10^6 cells/ml. For transformants HTC1 (Barth *et al.,* 1994), CPH (Beug, Katz, and Gerish, 1973), and T10 (Faix *et al.,* 1992), 20 μg/ml of the selection marker G418 was added to stabilize csA expression. Before measurements were taken, cells were washed and resuspended in 17 m*M* K/Na buffer, pH 6.0, and used either immediately as undeveloped cells or after shaking for about 6 h at 150 rpm as developed cells. The temperature was about 20°C. For the measurement, cells were suspended in 17 m*M* K/Na phosphate buffer, pH 6.0, and spread on polystyrene Petri dishes, 3.5 cm in diameter, at a density of about 100 cells/mm^2. To chelate Ca^{2+}, 5 m*M* ethylendiaminotetraacetic acid (EDTA) was added at pH 6.0 in the same buffer. To avoid laser beam scattering of the detection system, nonadherent cells were removed by gently rinsing the dish after 10 min.

V. Final Remarks

The two concepts of either monolayer interactions or single-cell interactions illuminate complementary aspects of the complex cellular adhesion mechanisms. By reducing the complexity, as in the case of measurements between individual *Dictyostelium* cells, processes on the single molecular level are resolved. And the principle of gaining adhesion strength by oligomerization of molecular binding partners can be assumed from these measurements. Insights into the complexity of molecular arrangements, during cell adhesion processes, become possible by the measurements between interacting monolayers.

Bond rupture experiments are performed under nonequilibrium conditions, thus the measured forces are rate dependent. As shown by several groups (Grubmüller *et al.,* 1995; Merkel *et al.,* 1999; Rief *et al.,* 1998), this rate dependence may reveal additional information on the binding potential. For living cells this detailed analysis will be important to relate cell adhesion to the rate of cell movement or shear forces in the blood stream (Chen and Springer, 1999).

The combination of nanophysics with cell biology establishes a mechanical assay that relates qualitatively cooperative molecular processes during contact formation, or even quantitatively the expression of a gene, to the function of its product in cell adhesion. This type of single-molecule force spectroscopy on live cells is directly applicable to a variety of different cell adhesion systems. A wide field of applications of this cell-based molecular assay is predictable, for instance, in investigating mutated cell adhesion proteins or coupling of cell adhesion molecules to the cytoskeleton and also in the evaluation of adhesion-blocking drugs. Furthermore, not only initial steps in the receptor-mediated adhesion of particles to phagocyte surfaces but also interaction of cells with natural and artificial surfaces of medical interest can be measured with this technique.

Acknowledgments

This work became possible only through collaborations with M. Thie, R. Röspel, B. Maranca-Nowak, and U. Trottenberg at the Uni-Klinikum Essen in H.-W. Denker's institute; D. Gabriel, E. Simmeth, and M. Westphal at the MPI-Martinsried in G. Gerisch's institute; M. Grandbois at the University of Missouri-Columbia; and W. Dettmann, A. Wehle, and A. Kardinal in the LMU München at H. E. Gaub's institute. We are also grateful to the Deutsche Forschungsgemeinschaft and the Volkswagenstiftung for funding.

References

Albers, A., Thie, M., Hohn, H.-P., and Denker, H.-W. (1995). Differential expression and localization of integrins and CD44 in the membrane domains of human uterine epithelial cells during the menstrual cycle. *Acta Anatom.* **153,** 12–19.

Barth, A., Müller-Taubenberger, A., Taranto, P., and Gerisch, G. (1994). Replacement of the phospholipid-anchor in the contact site A glycoprotein of *Dictyostelium discoideum* by a transmembrane region does not impede cell adhesion but reduces residence time on the cell surface. *J. Cell Biol.* **124,** 205–215.

Baumgartner, W., Hinterdorfer, P., Ness, W., Raab, A., Vestweber, D., Schindler, H., and Drenckhahn, D. (2000). Cadherin interaction probed by atomic force microscopy. *PNAS* **97,** 4005–4010.

Benoit, M., Gabriel, D., Gerisch, G., and Gaub, H. E. (2000). Discrete molecular interactions in cell adhesion measured by force spectroscopy. *Nature Cell Biol.* **2,** 313–317.

Beug, H., Katz, F. E., and Gerisch, G. (1973). Dynamics of antigenic membrane sites relating to cell aggregation in *Dictyostelium discoideum*. *J. Cell Biol.* **56,** 647–688.

Beug, H., Katz, F. E., Stein, A., and Gerisch, G. (1973). Quantitation of membrane sites in aggregating Dictyostelium cells by use of tritiated univalent antibody. *Proc. Natl. Acad. Sci. U.S.A.* **70,** 3150–3154.

Binnig, G., Quate, C. F., and Gerber, C. (1986). Atomic force microscope. *Phys. Rev. Lett.* **56,** 930–933.

Bruinsma, R., Behrisch, A., and Sackmann, E. (2000). Adhesive switching of membranes: Experiment and theory. *Phys. Rev. E.* **61,** 4253–4267.

Chen, A., and Moy, V. T. (2000). Cross-linking of cell surface receptors enhances cooperativity of molecular adhesion. *Biophys. J.* **78,** 2814–2833.

Chen, S., and Springer, T. A. (1999). An automatic breaking system that stabilizes leukocyte rolling by an increase in selectin bond number with shear. *J. Cell Biol.* **144,** 185–200.

Choquet, D., Felsenfeld, D. P., and Sheetz, M. P. (1997). Extracellular matrix rigidity causes strengthening of integrin-cytoskeleton linkages. *Cell* **88,** 39–48.

Curtis, A. S. G. (1970). Problems and some solutions in the study of cellular aggregation. *Symp. Zool. Soc. London* **25,** 335–352.

Dai, J., and Sheetz, M. P. (1998). Cell membrane mechanics. *In* "Methods Cell Biology," (M. P. Sheetz, ed.), Vol. 55, pp. 157–171. Academic Press, San Diego.

Denker, H.-W. (1994). Endometrial receptivity: cell biological aspects of an unusual epithelium. *Ann. Anat.* **176,** 53–60.

Dettmann, W., Grandbois, M., Andrè, S., Benoit, M., Wehle, A. K., Kaltner, H., Gabius, H.-J., and Gaub, H. E. (2000). Differences in zero-force and force-driven kinetics of ligand dissociation from β-galactoside-specific proteins (plant and animal lectins, immunoglobulin G) monitored by plasmon resonance and dynamic single molecule force microscopy. *Arch. Biochem. Biophys.* **383,** 157–170.

Domke, J., Dannöhl, S., Parak, W. J., Müller, O., Aicher, W. K., and Radmacher, M. (2000). Substrate Dependent Differences in Morphology and Elasticity of Living Osteoblasts Investigated by Atomic Force Microscopy. *Colloids Surf. B Biointerfaces,* **19,** 367–379.

Evans, E. A. (1985). Detailed mechanics of membrane-membrane adhesion and separation II. Discrete kinetically trapped molecular cross-bridges. *Biophys. J.* **48,** 185–192.

Evans, E. (1995). Physical Actions in Biological Adhesion. *In* "Handbook of Biological Physics," (R.a.S., E. Lipowsky, ed.), Vol. 1B, pp. 723–754. Elsevier Science Amsterdam.

Evans, E., and Ritchie, K. (1997). Dynamic strength of molecular adhesion bonds. *Biophys. J.* **72,** 1541–1555.

Faix, J. (1999). Contact site A. *In* Guidebook to the Extracellular Matrix, Anchor, and Adhesion Proteins (T.K.a.R. Vale, ed.), Oxford Univ. Press, London.

Faix, J., Gerisch, G., and Noegel, A. A. (1992). Overexpression of the csA cell adhesion molecule under its own cAMP-regulated promoter impairs morphogenesis in *Dictyostelium. J. Cell Sci.* **102,** 203–214.

Felsenfeld, D. P., Choquet, D., and Sheetz, M. P. (1996). Ligand binding regulates the directed movement of betal integrins on fibroblasts. *Nature* **383,** 438–440.

Florin, E.-L., Moy, V. T., and Gaub, H. E. (1994). Adhesive forces between individual ligand-receptor pairs. *Science* **264,** 415–417.

Fritz, M., Radmacher, M., and Gaub, H. E. (1993). In vitro activation of human platelets triggered and probed by SFM. *Exp. Cell Res.* **205**(1), 187–190.

Gimzewski, J. K., and Joachim, C. (1999). Nanoscale science of single molecules using local probes. *Science* **283,** 1683–1688.

Goldmann, W. H., Galneder, R., Ludwig, M., Kromm, A., and Ezzell, R. (1998). Differences in F9 and 5.51 cell elasticity determined by cell poking and atomic force microscopy. *FEBS Lett.* **424,** 139–142.

Grandbois, M., Beyer, M., Rief, M., Clausen-Schaumann, H., and Gaub, H. E. (1999). How strong is a covalent bond? *Science* **283,** 1727–1730.

Grandbois, M., Dettmann, W., Benoit, M., and Gaub, H. E. (2000). Affinity imaging of red blood cells using an atomic force microscope. *J. Histochem. Cytochem.* **48,** 719–724.

Grubmüller, H., Heymann, B., and Tavan, P. (1995). Ligand binding: molecular mechanics calculation of the streptavidin-biotin rupture force. *Science* **271,** 997–999.

Harloff, C., Gerisch, G., and Noegel, A. A. (1989). Selective elimination of the contact site A protein of *Dictyostelium discoideum* by gene disruption. *Genes Dev.* **3,** 2011–2019.

Hinterdorfer, P., Baumgartner, W., Gruber, H. J., Schilcher, K., and Schindler, H. (1996). Detection and localization of individual antibody-antigen recognition events by atomic force microscopy. *Proc. Natl. Acad. Sci. U.S.A.* **93,** 3477–3481.

Hochmuth, R. M., Shao, J.-Y., Dai, J., and Sheetz, M. P. (1996). Deformation and flow of membrane into tethers extracted from neuronal growth cones. *Biophys. J.* **70,** 358–369.

Hoh, J. H., and Schoenenberger, C.-A. (1994). Surface morphology and mechanical properties of MDCK monolayers by atomic force microscopy. *J. Cell Sci.* **107,** 1105–1114.

Holmberg, M., Wigren, R., Erlandsson, R., and Claesson, P. M. (1997). Interactions between cellulose and colloidal silica in the presence of polyelectrolytes. *Colloids Surf. A Physicochem. Eng. Aspects* **129–130,** 175–183.

John, N., Linke, M., and Denker, H.-W. (1993). Quantitation of human choriocarcinoma spheroid attachment to uterine epithelial cell monolayers. *In Vitro Cell. Dev. Biol.* **29A,** 461–468.

Johnsson, B., Löfas, S., and Lindquist, G. (1991). Immobilization of proteins to a carboxymethyldextran-modified gold surface for biospecific interaction analysis in surface plasmon resonance sensors. *Anal. Biochem.* **198,** 268–277.

Kamboj, R. K., Wong, L. M., Lam, T. Y., and Siu, C.-H. (1988). Mapping of a cell-binding domain in the cell adhesion molecule gp80 of Dictyostelium discoideum. *J. Cell Biol.* **107,** 1835–1843.

Kreis, T., and Vale, R. (eds.) (1999). "Guidebook to the Extracellular Matrix, Anchor, and Adhesion Proteins." Oxford Univ. Press, London.

Kuo, S. C., Hammer, D. A., and Lauffenburger, D. A. (1997). Simulation of detachment of specifically bound particles from surfaces by shear flow. *Biophys. J.* **73,** 517–531.

Kuramoto, H., Tamura, S., and Notake, Y. (1972). Establishment of a cell line of human endometrial adenocarcinoma in vitro. *Am. J. Obstet. Gynecol.* **114,** 1012–1019.

Malchow, D., Nägele, B., Schwarz, H., and Gerisch, G. (1972). Membrane-bound cyclic AMP phosphodiesterase in chemotactically responding cells of *Dictyostelium discoideum*. *Eur. J. Biochem. Eur. J. Biochem.* **28,** 136–142.

Marszalek, P. E., Pang, Y. P., Li, H., Yazal, Y. E., Oberhauser, A. F., and Fernandez, J. M. (1999). Atomic levers control pyranose ring conformations. *Proc. Natl. Acad. Sci. U.S.A.* **96**.

Merkel, R., Nassoy, P., Leung, A., Ritchie, K., and Evans, E. (1999). Energy landscapes of receptor-ligand bonds explored with dynamic force spectroscopy. *Nature* **397,** 50–53.

Müller, K. M., Arndt, K. M., and Plückthun, A. (1988). Model and simulation of multivalent binding to fixed ligands. *Anal. Biochem.* **261,** 149–158.

Müller, D. J., Baumeister, W., and Engel, A. (1999). Controlled unzipping of a bacterial surface layer with an AFM, Nov 9:96 (23), p. 13170–13174. PNAS.

Murray, B. A., Yee, L. D., and Loomis, W. F. (1981). Immunological analysis of glycoprotein (contact sites A) involved in intercellular adhesion of Dictyostelium discoideum. *J. Supramol. Struct. Cell. Biochem.* **17,** 197–211.

Oberhauser, A. F., Marszalek, P. E., Erickson, H. P., and Fernandez, J. M. (1998). The molecular elasticity of the extracellular matrix protein tenascin. *Nature* **393,** 181–185.

Oesterhelt, F., Oesterhelt, D., Pfeiffer, M., Engel, A., Gaub, H. E., and Müller, D. J. (2000). Unfolding pathways of individual Bacteriorhodopsins. *Science* **288,** 143–146.

Patillo, R. A., Ruckert, A., Hussa, R., Bernstein, R., and Delfs, E. (1971). The JAR cell line—Contiuous human multihormone production and controls. *In Vitro* **6,** 398.

Ponte, E., Bracco, E., Faix, J., and Bozzaro, S. (1998). Detection of subtle phenotypes: The case of the cell adhesion molecule csA in Dictyostelium. *Proc. Natl. Acad. Sci. U.S.A.* **95,** 9360–9365.

Radmacher, M. (1997). Measuring the elastic properties of biological samples with the atomic force microscopy. *IEEE Eng. Med. Biol.* **16.**

Radmacher, M., Fritz, M., Kacher, C. M., Cleveland, J. P., and Hansma, P. K. (1996). Measuring the viscoelastic properties of human platelets with the atomic force microscope. *Biophys. J.* **70,** 556–567.

Razatos, A., Ong, Y.-L., Sharma, M. M., and Georgiou, G. (1998). Molecular determinats of bacterial adhesion monitored by AFM. *PNAS* **95,** 11,059–11,064.

Rief, M., Clausen-Schaumann, H., and Gaub, H. E. (1999). Sequence dependent mechanics of single DNA-molecules. *Nature Struct. Biol.* **6,** 346–349.

Rief, M., Fernandez, J. M., and Gaub, H. E. (1998). Elastically coupled two-level systems as a model for biopolymer extensibility. *Phys. Rev. Lett.* **81,** 4764–4767.

Rief, M., Gautel, M., Oesterhelt, F., Fernandez, J. M., and Gaub, H. E. (1997). Reversible unfolding of individual titin Ig-domains by AFM. *Science* **276,** 1109–1112.

Rief, M., Oesterhelt, F., Heymann, B., and Gaub, H. E. (1997). Single molecule force spectroscopy on polysaccharides by AFM. *Science* **275,** 1295–1298.

Sagvolden, G., Giaver, I., Pettersen, E. O., and Feder, J. (1999). Cell adhesion force microscopy. *Proc. Natl. Acad. Sci. U.S.A.* **96,** 471–475.

Smith, B. L., Schäffer, T. E., Viani, M., Thompson, J. B., Frederick, N. A., Kindt, J., Belcher, A., Stucky, G. D., Morse, D. E., and Hansma, P. K. (1999). Molecular mechanistic origin of the toughness of natural adhesives, fibres and composites. *Nature* **399,** 761–763.

Springer, T. A. (1990). Adhesion receptors of the immune system. *Nature* **346,** 425–434.

Stadler, J., Keenan, T. G., Bauer, G., and Gerisch, G. (1989). The contact site A glycoprotein of *Dictyostelium discoideum* carries a phospholipid anchor of a novel type. *EMBO J.* **8,** 371–377.

Strunz, T., Oroszlan, K., Schäfer, R., and Güntherodt, H.-J. (1999). Dynamic force spectroscopy of single DNA molecules. *Proc. Natl. Acad. Sci. U.S.A.* **96,** 11,277–11,282.

Suter, C. M., Errante, L. E., Belotserkovsky, V., and Forscher, P. (1998). The Ig superfamily cell adhesion molecule, apCAM, mediates growth cone steering by substrate-cytoskeletal coupling. *J. Cell Biol.* **141,** 227–240.

Thie, M., Fuchs, P., Butz, S., Sieckmann, F., Hoschützky, H., Kemler, R., and Denker, H.-W. (1996). Adhesiveness of the apical surface of uterine epithelial cells: The role of junctional complex integrity. *Eur. J. Cell Biol.* **70,** 221–232.

Thie, M., Harrach-Ruprecht, B., Sauer, H., Fuchs, P., Albers, A., and Denker, H.-W. (1995). Cell adhesion to the apical pole of epithelium: a function of cell polarity. *Eur. J. Cell Biol.* **66,** 180–191.

Thie, M., Herter, P., Pommerenke, H., Dürr, F., Sieckmann, F., Nebe, B., Rychly, J., and Denker, H.-W. (1997). Adhesiveness of the free surface of a human endometrial monolayer as related to actin cytoskeleton. *Mol. Hum. Reprod.* **3,** 275–283.

Thie, M., Röspel, R., Dettmann, W., Benoit, M., Ludwig, M., Gaub, H. E., and Denker, H.-W. (1998). Interactions between trophoblast and uterine epithelium: Monitoring of adhesive forces. *Hum. Reprod.* **13,** 3211–3219.

Tomschy, A., Fauser, C., Landwehr, R., and Engel, J. (1996). Homophilic adhesion of E-cadherin occurs by a co-operative two-step interaction of N-terminal domains. *EMBO J.* **15,** 3507–3514.

Vestweber, D., and Blanks, J. E. (1999). Mechanisms that regulate the function of the selectins and their ligands. *Physiological Rev.* **79,** 181–213.

Ward, M. D., Dembo, M., and Hammer, D. A. (1994). Kinetics of cell detachment: Peeling of discrete receptor clusters. *Biophys. J.* **67,** 2522–2534.

Ward, M. D., and Hammer, D. A. (1993). A theoretical analysis for the effect of focal contact formation on cell-substrate attachment strength. *Biophys. J.* **64,** 936–959.

Way, D. L., Grosso, D. S., Davis, J. R., Surwit, E. A., and Christian, C. D. (1983). Characterization of a new human endometrial carcinoma (RL95-2) established in tissue culture. *In Vitro* **19,** 147–158.

Willemsen, O. H., Snel, M. M. E., van der Werf, K. O., de Grooth, B. G., Greve, J., Hinterdorfer, P., Gruber, H. J., Schindler, H., van Kooyk, Y., and Figdor, C. G. (1998). Simultaneous height and adhesion imaging of antibody-antigen interactions by atomic force microscopy. *Biophys. J.* **75,** 2220–2228.

Yauch, R. L., Felsenfeld, D. P., Kraeft, S.-K., Chen, L. B., Sheetz, M. P., and Hemler, M. E. (1997). Mutational evidence for control of cell adhesion through integrin diffusion/clustering, independent of ligand binding. *J. Exp. Med.* **186,** 1347–1355.

Zahalak, G. I., McConnaughey, W. B., and Elson, E. L. (1990). Determination of cellular mechanical properties by cell poking, with an application to leukocytes. *J. Biomech. Eng.* **112,** 283–294.

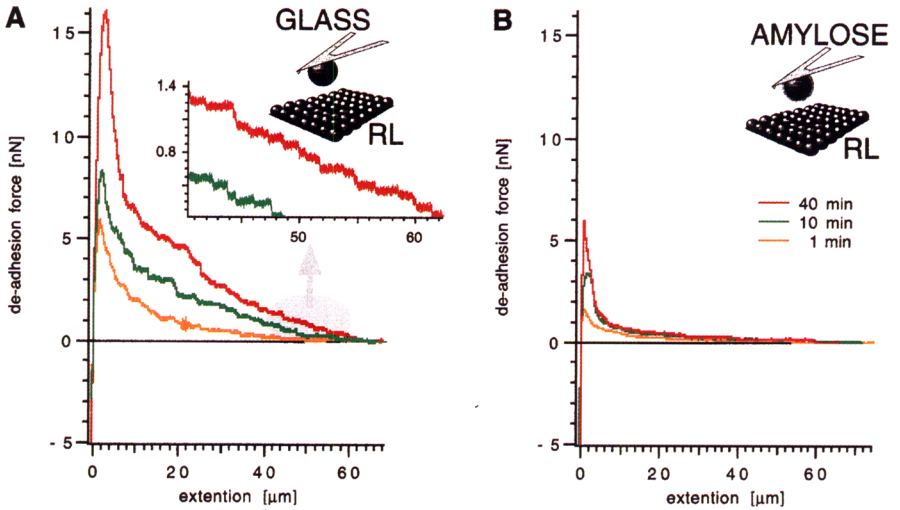

Fig. 5.5 Two sets of deadhesion force traces recorded with a plain glass surface on the sensor (A) and an amylose-passivated surface (B) after contacts of 1, 10, and 40 min at 5 nN on a confluent monolayer of epithelial cells (RL95-2). The contact area was about 500 μm^2. Inset (A) zooms into the traces where indicated by the circle revealing single rupture steps (Thie *et al.,* 1988).

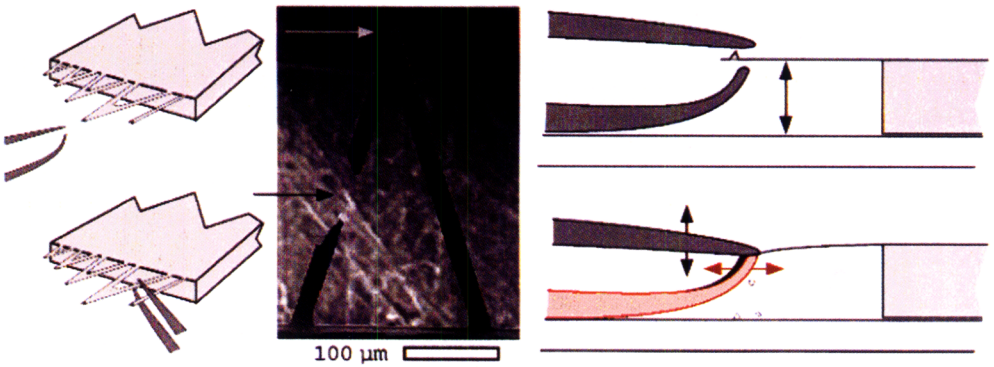

Fig. 5.8 Scheme of the "surgery" on a cantilever with tweezers and a SEM image of such a sensor.